

Knowledge-Based Adaptive Stagger-Block-Lattice-Filter MTI Processor


Xubao Zhang^{1,2,*}

ABSTRACT

This paper researches adaptive stagger-block-lattice-filter (SBLF) processor, which can be applied to an MTI radar. Our years' experiments prove the necessity to incorporate AI into the processor. Only algorithmic operation largely restricts clutter suppression performance in complex environments. The high speed and small radar-cross-section of a target compel an MTI to be upgraded by stagger pulse repetition interval (PRI), pulse compression (PC) transmission, and intelligent operation. Five heuristic strategies for the adaptive SBLF processor are proposed: 1) non-clutter block decision and threshold set-up, which decides whether the Test block to be dominated by a clutter and uses the filtering-itself output to set up detection thresholds; 2) Target block identification and PC terrace-indication declaration, which identifies the Test block to be dominated by a target or clutter and determines the terrace-indication; 3) SBLF coefficient estimation, which calculates SBLF coefficients in the Guard I block in real-time; 4) Establishment of clutter-map, which stores the thresholds, target block index, terrace-indication index, SBLF coefficients, and notch parameters in the corresponding map cells; 5) Guidance of stagger PRI, which collects target block indices on adjacent bearing bins and notch parameters to maximize target acquisition and to suggest the available PRI. In order to verify effectiveness of the above intelligent operations, we have done a lot experiments with computer and selected a ship-borne radar as the background; the clutter returns feature the land, sea and weather environments, and the target returns feature weak high-speed aircrafts. In homogeneous and heterogeneous clutters, this processor demonstrates the individual ability to acquire the weak targets in the strong clutter.

Submitted: June 04, 2025

Published: September 15, 2025

 10.24018/ejai.2025.4.5.74

¹Xi'an Electronic and Scientific, Technology University, China.

²Unitron, Sonova, Canada.

*Corresponding Author:
e-mail: xbzwdl@yahoo.com

Keywords: Adaptive processor, artificial intelligence, lattice filter, MTI.

1. INTRODUCTION

Based on stationarity process assumption, many literatures to study adaptive filters describe the optimization theories, which are restricted within numerical operations [1], [2]. In the early 1980s, references Thurber [3], Gaby and Hayes [4] and Gass *et al.* [5] introduced practical adaptive radar systems and spectrum estimation, and had incorporated some nonnumerical operations due to reasoning requirements; actually, those were just a class of primary intelligent operations. Because of the technology limitations and low-level devices, those radars' adaptive track speeds were not fast and the reasoning strategies were not complete. By the 21st century, AI in signal processing is rapidly developed, it associates with the speech recognition, navigation and radar systems, etc. [6]–[8]. Melvin

and Guerri [7] employed the measured data from radar programs to illustrate realistic effects limiting radar performance. Then, they examine intelligent training methods to enhance space-time adaptive detection performance. The training data can not contain the clutter and it is a crucial step to realize them to estimate the adaptive weights; they described this issue in detail.

Speeds of modern aircrafts and missiles are extremely high, up to Mach 3 or larger, then the radial speed range may also reach the number. No matter a uniform-PRI is selected to be low, medium or high, they always cause speed-ambiguity or/and range-ambiguity. Stagger PRI pulse transmission is commonly used to solve the speed-ambiguous [9]. Large time-width PC is also involved in MTI radar for low pulse transmission power, high range resolution, electronic support measures, etc. [10]. Thus,



the adaptive MTI processor always incorporates the both features. An adaptive filter usually can produce its coefficients in two ways: one is to design them in advance with the match or eigenvector algorithm and to store them in weight-base; the other is to calculate them in real-time with the lattice algorithm. Based on many years' study on adaptive filtering for MTI system, we propose block lattice filter algorithm [11], which calculates the coefficients with range \times bearing block data from the stagger-PRI returns and performs optimal improvement factor as the lattice with uniform PRI does in the stationary clutters. The resulting filter is called the stagger-block-lattice-filter (SBLF). In addition, this structure has low computation load and low sensitivity of operator word length in comparing with the transversal filter structure, so it is easily implemented in a real-time filtering processor. In practical simulation, the experimental conditions are to be created under as realistic environments and compatible with the technologies. This paper intends to describe necessity to incorporate intelligent operations into the adaptive SBLF MTI processor and to introduce the heuristic strategies based on priori knowledges, and then we expose some experiments results to illustrate the excellent and good performances of the processor under the conditions of homogeneous and heterogeneous clutters, respectively.

2. PRIOR KNOWLEDGES OF THE INTELLIGENT SBLF PROCESSOR

The so-called knowledges mean radar professionals' knowledges. The following is basic knowledges adopted by the processor.

2.1. Reasoning Construction of the SBLF Processor

Aircraft and missile returns (targets) or land and weather returns (clutters) from coherent pulses emitted by an MTI radar are correlated over adjacent CPI (coherent processing interval) samples but their Doppler frequencies are different. This builds MTI processor foundation. For EM counter-measurement, stealth aircraft and high-speed missile are developed rapidly. Generally, a target's radar-cross-section (RCS) is small and its return power is weak; a clutter return has a very large RCS and submerges targets. Thus, the processor aims at strong clutter suppression and weak target acquisition, and also incorporates the stagger PRI and large time-width PC features. Theoretically the optimal filter algorithms can reach excellent performance of 50 dB or larger improvement factor [11], [12]. In practice, such performances of the optimal filters are compromised due to clutter heterogeneity and multi technologies' involution. For example, to prevent the target from being filtered out, the processor has to estimate the SBLF coefficients in a data block where no target presents, referred as training block. The crucial problem is how we can realize it. Thus, the first operation for this processor to do is not numerical arithmetic like $y = F(x)$ but rather reasoning operation like "If, then," specifically, learning, identification, decision, etc. As soon as the training block are realized, the SBLF coefficients are easily calculated without mismatch, then used to filter the next block data. This way is the common delaying-and-filtering.

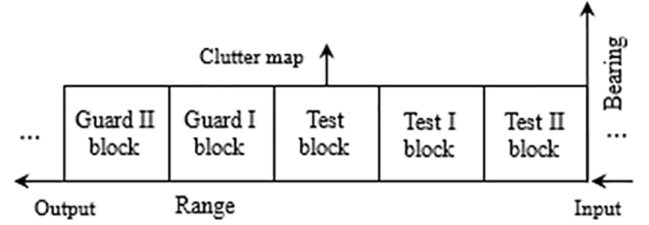


Fig. 1. Reasoning center of the adaptive SBLF processor.

In the experiments below, one data array is divided into multi blocks, one block is composed of data of $L_r \times N_b$, L_r length of the range bins and N_b number of the bearing bins, in this paper $N_b = 7$ always. When a string of blocks enters the processor, its several blocks carry out together SBLF filtering with relevant intelligent operations and are called the reasoning center. Fig. 1 shows the center composed of five blocks; Guard II and I blocks are ahead of Test block and are used to estimate SBLF coefficients when the training data present inside; Test I and II blocks are behind of Test block and are always used to filter with the SBLF. The Test block is used to filter, estimate, or investigate, and sends out the resulting information data to clutter-map. This processing is repeated as the successive blocks' data are entering.

2.2. Performance Behaviors of Three Filtering Modes

Now we do an experiment with three different filtering modes. Two-clutter plus two-target return array of 240 range bins \times 7 bearing bins is divided into 12 blocks of length 20 bins; 5 and 30 dB targets are placed in bins 41 and 151, respectively. When adjacent blocks' data enter the reasoning center of Fig. 1, they are regarded as Guard II, I, Test and Test I, II blocks in turn. ① One-block data of Test, Test I or II are used to estimate SBLF coefficients, which are used to filter their individual block data, the mode is called estimating- and filtering-itself or filtering-itself for short. ② The SBLF coefficients are calculated with Guard I block data and are used to filter Test block data, the mode is called block-delayed filtering. ③ The SBLF coefficients are calculated in Guard I block and the data of Test, Test I and II blocks are filtered with the coefficients, the mode is called terrace-delay filtering. Fig. 2 shows the test results from the SBLF processor and the three modes perform their individual behaviors. The parameters of the land plus cloud clutters are:¹ P_g 60 dB, F_g 12 Hz, D_g 7.2 Hz and P_w 10 dB, F_w 240 Hz, D_w 58 Hz and the target parameters are listed on the figure top. The white noise power is normalized to 0 dB. The black curve denotes the power of SBLF input, fluctuating around 60 dB; the blue curve, the power of SBLF output in filtering-itself mode, fluctuating around 12 dB, which does not reveal any target cue; the red curve, the power of SBLF output in block-delay filtering mode, covered partially by green but two target cues appear, one is a weak step from bins 41 to 60, fluctuating around 21 dB and the other is a regular step from bins 151 to 160 about

¹In this paper, all the clutters are modeled as Gaussian spectrum. P_g , P_w , and P_s denote powers of land, weather (cloud or raining), and sea clutters, respectively; F_g , F_w , and F_s denote center frequencies of the three-class clutters, respectively; D_g , D_w , and D_s denote standard variance bandwidths of the three-class clutters, respectively. The target is modeled as point-frequency spectrum. P_t and F_t denote its power and frequency, respectively.

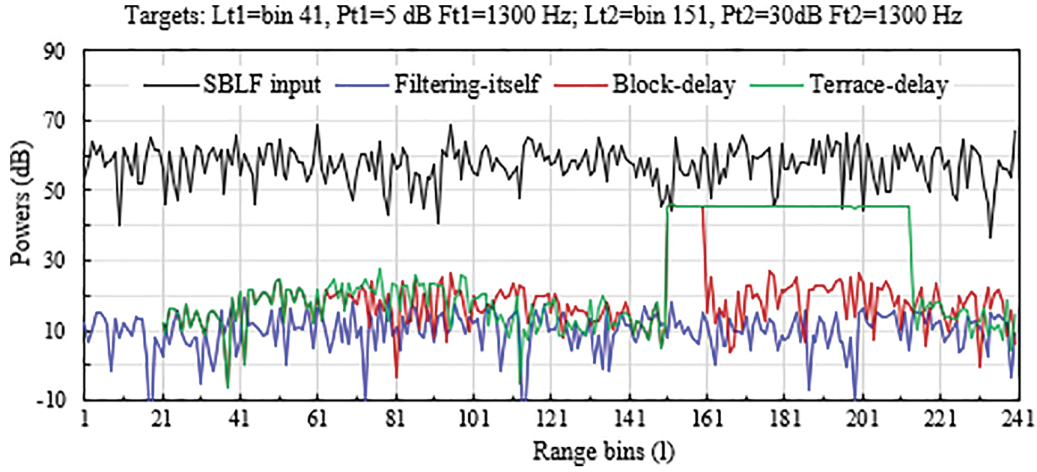


Fig. 2. Performance behaviors of three filtering modes of the SBLF processor in a homogenous clutter.

45 dB; the clutters at both sides of target-steps are fluctuating around 20 dB; there is no data from bins 1 to 20 due to no filtering. The green curve, the output power of terrace-delay filtering, two target terrace-indications appear on it and each length occupies 63 bins; one is the irregular terrace, about 21 dB high, from bins 41 to 103 and the other is the regular terrace, about 45 dB high from bins 151 to 213, the clutters at both sides of the terrace are fluctuating around 17 dB. These test results indicate that for a PC target the terrace-delay filtering mode provides remarkable cues as the block-delay filtering mode performs. This is one key priori knowledge of the SBLF processing.

2.3. Adaptive Detection Threshold

From the blue curve in Fig. 2, no matter the targets are weak 5 dB or non-weak 30 dB, the filtering-itself output of the SBLF is no target cue and is relatively stable. Utilizing the filtering behavior in a homogeneous clutter, we can use the filtering-itself output to set up target detection thresholds; when comparing the blue curve with the red SBLF output, the processor easily determines if a target presents in Test block. In the case of a PC target, if the green output of the Test block exceeds a threshold determined by the blue outputs of Guard I, Test, and Test I blocks, a PC target is acquired in Test block. So, it is a great finding for setting up adaptive threshold with the filtering-itself outputs and the adaptivity also increase detection sensitivity, i.e., beneficial to weak target acquisition. Specifically, we take average of the blue output magnitudes O_{GI} , O_T , O_{TI} of the Guard I, Test, and Test I, i.e.,:

$$T_D = (O_{GI} + O_T + O_{TI})/3 \quad (1)$$

and call the average value T_D the output threshold to detect a target. Additionally, a threshold factor F_T from 1.5 to 2.5, is also selected to control the detection sensitivity. Product of T_D multiplied by F_T , $T_{Da} = F_T T_D$, is called the adaptive threshold. Later we use T_{Da} to detect targets in the homogeneous clutter; this is a simple reasoning in adaptive clutter suppression but its effectiveness is quite remarkable. When a PC target is presenting, usually the SBLF output terrace appears on the adjacent blocks, e.g., Test, Test I and II; however, when the target signal is corrupted or

in a heterogeneous clutter, the terrace-indication may be irregular. As long as the target is declared in Test block, the block data are no longer used as training data and the coefficients from Guard I block are maintained until the terrace-indication ends.

In the case of heterogeneous clutters, since statistics of the clutter are unstable, the formula (1) may need more filtering-itself blocks to calculate the output threshold.

2.4. Multiple Stagger PRIs

This SBLF processor involves the stagger low PRI, which makes the frequency/speed response period extended by many times larger than that response period of the low uniform-PRI, then the MTI overcomes speed-ambiguity disadvantage. For example of an S-band radar of 3 GHz, assume that an aircraft speed is close to Mach 1, then its Doppler frequency is at highest 6.86 kHz. If the uniform PRF is 720 Hz, there are 9.53 ambiguous speeds within this Mach. However, when a stagger-PRI of average PRF 720 Hz is utilized and its stagger code is from seven integers, 26, 27, 28, 29, 30, 31, 32, the frequency period extension is 29 and the corresponding stagger PRIs are 1.25, 1.29, 1.34, 1.39, 1.44, 1.49, 1.53 ms. In order to get the shallowest notches, the integer code needs to be rearranged by a mathematical programming [12]. For example, the rearranged code 27 26 31 29 30 28 32 has the PRIs 1.29, 1.25, 1.49, 1.39, 1.44, 1.34, 1.53 ms and the deepest notch is 0.97 dB within five times the average PRF. The improvement of signal-to-clutter ratio (SCR) of the SBLF is impacted when the Doppler frequency drops into the notches. The average SCR improvement factor can reach 53 dB; when the notch depth is -5 dB, the improvement of a target dropping the notch will be 48 dB only; it is impossible to acquire a weak target from a strong clutter. So, it is necessary for the SBLF processor to check the notches after the SBLF coefficients are calculated.

Generally, the given frequency response notches are the result of analytic calculation, i.e., using the non-real-time filter coefficients, they are not in practice. In real-time adaptive processing, the coefficients and notches both are calculated in real-time instead of the analytic. For example, we give a clutter environment, P_g 55 dB, F_g 12 Hz, D_g 7.2 Hz, and P_w 20 dB, F_w 240 Hz, D_w 58 Hz. Using the

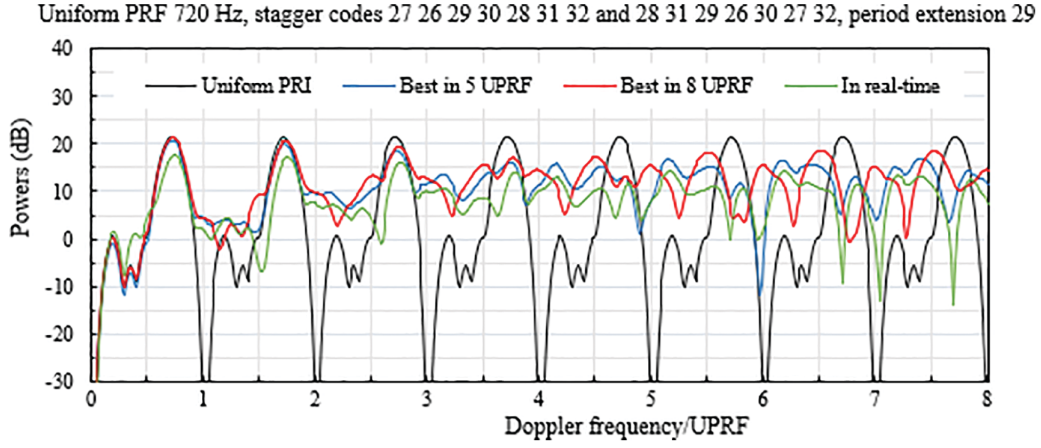


Fig. 3. Frequency responses of the SBLF processor with uniform and stagger PRIs.

stagger PRI parameters in the last paragraph, we calculate frequency responses under the different conditions: ① the uniform PRI 1/720 s, its period code is 29 29 29 29 29 29 29; ② one stagger PRI, it has the shallowest notch within five times the average PRF, the code is 27 26 31 29 30 28 32; ③ the other stagger PRI, it has the shallowest notch within eight times the average PRF, the code is 28 31 29 26 30 27 32; ④ the real-time SBLF coefficients, its stagger PRI is the same as in ③. Fig. 3 shows their frequency responses within a frequency range up to 5.76 kHz, for a flight of Mach 0.84; they are denoted by black, blue, red, and green curves, respectively. We observe that the black curve badly performs eight deep notches, lower than -30 dB at multiples of the average PRF, we can not see the target dropping into such a notch even if it is strong, larger than 40 dB; the blue curve has the deepest drop, 0.97 dB at 3.5 kHz; the red curve has the deepest drop -2.25 dB at 0.83 kHz; the green curve has the deepest drop -6.85 dB at 1.1 kHz. The three stagger PRIs perform much shallower notches than those of the uniform PRI, so they can really alleviate improvement factor loss. The notches of real-time coefficients are deeper than those of analytic coefficients, and the real-time SBLF with large average number can approach to the analytic results. In the practical simulation, checking the notches and guiding the stagger PRI of the MTI can assist to acquire the weak target.

3. HEURISTIC STRATEGIES OF THE SBLF PROCESSOR

In practical simulating, the intelligent operations of the SBLF processor are more complex than the knowledges above. The clutter returns may be heterogeneous, e.g., the environment may be a combination of varying discrete clutters. So how all the collected priori knowledges are incorporated into the SBLF processor refers to more reasonings: learning, analyzing, examination, correcting, and memorizing. For example, in the entire environment, whether the SBLF needs to be enabled, how the processor realizes the training block, how the target block is identified, how PC terrace-indication is declared, etc. Under the prerequisites: ① involvement with stagger PRI and phase-coded PC, ② two-dimensional return arrays of bearing x range, ③ clutter backgrounds of mountain, cloud, sea, and

raining, ④ the SBLF in reference [11] placed ahead of the PC, we proposed five heuristic strategies as follows.

3.1. Non-Clutter Input Identification and Adaptive Threshold Set-up

This strategy works in Test block first. When the input power is lower than 10 dB, we regard the input as non-clutter input, the SBLF is disabled in Test block and the input signal enters the PC processor directly. It is possible that a target presents in the low-level input. However, ① if the SBLF is enabled, it may cause a SCR loss due to frequency response notches; ② generally the target-detectable factor is SNR 8 dB at display screen and the value can be reached when the PC is enabled.

Given a complex input $\{x_c(t_n, l)\}$, $n \in \{0, 1, \dots, N_b-1\}$, N_b number of bearing bins and $l \in \{1, 2, \dots, L_r\}$, L_r block length; CPIs of the same range bins, $\{t_n\}$, are stagger. After filtering-itself in Guard I, Test, and Test I blocks, the outputs $\{y_c(t_n, l)\}$ are used to set up the detection thresholds. The average output magnitude of Test block is calculated as

$$O_T = \sum_{l=1}^{L_r} \sum_{n=0}^{N_b-1} [y_c(t_n, l) y_c^*(t_n, l)]^{1/2} / N_b / L_r \quad (2)$$

The three output magnitudes O_{GI} , O_T , and O_{TI} from (2) here are averaged in terms of (1), then the output threshold T_D and adaptive threshold T_{Da} can be obtained. In the heterogeneous clutter, using (1) to set up the detection threshold is still effective because the environment is locally homogeneous but more blocks of filtering-itself and position-symmetric may be required, e.g., Guard II, I, Test, Test I, II blocks. The threshold factor, F_T , is selected to be larger and the detection sensitivity will be lower, but the false target rate is controlled. In fact, in a whole antenna scan, the F_T has to be selected as multi different values, depending on the clutter distribution of radar site.

3.2. Target Block Identification and Terrace-indication Declaration

This strategy works in four blocks Guard I, Test, Test I, II of Fig. 1. When the SBLF processor suppresses clutters and detects targets, the SBLF coefficients have to characterize the clutter only; otherwise, the SBLF may filter out both the clutter and target. At the SBLF input end,

the weak target is submerged and is no way recognized; however, after delay-filtering, the powers of the target and clutter are changed inversely and the target is easily identified. From the experiment in Fig. 2, we know that the block-delay filtering output reveals the target cues; when we use the coefficients from Guard I with training data to filter the data of Test block, the step-like target waveforms appear at its output. The block with a step-output is called the target block and its index is set as 1; inversely the block without a step-output, called clutter block, its index is set as 0. When the adjacent blocks, Test, Test I and Test II all are target blocks, the combined waveforms look like a terrace, called the terrace-indication. In machine learning, the processor compares the Test block output with the adaptive threshold and records the index. When the sum N_{ai} of the adjacent blocks' indices is equal to $\text{Mod}(L_{PC}/L_r) + 1$, L_{PC} PC length, the terrace-indication is declared and the blocks' data are not realized as training data. From Fig. 2, we also observe that when a weak target of 5 dB presents, the terrace-like waveform is irregular due to clutter corruption, but when non-weak target of 30 dB presents, the terrace-indication is very regular. How does this strategy help the processor identify PC target blocks? When index sum N_{ai} is counted to three or two, the PC target presence has a large probability and the terrace-indication is declared; when N_{ai} is one, the PC target presence has a little probability. After the terrace-indication is declared, the block following Test II is regarded as a clutter block; when its data enter the Guard I block, the block data are realized as training data. This strategy is reliable in a homogeneous clutter due to stationary statistics.

In a heterogeneous clutter, a strong clutter in a block may severely corrupt a target inside or may have higher level than the clutter in adjacent blocks, then, the target may be missing or the clutter may be declared as a "target." The number of filtering-itself blocks and the different threshold factor can adjust the adaptive threshold to alleviate the deterioration.

3.3. SBLF Coefficient Estimation

In the Guard I block we calculate the SBLF coefficients to reflect the clutter characteristic in Test block. When a target does not present in a block that has been declared as target index 0 or a block just following the declared terrace-indication, its data are moved to Guard I block. The data of Guard I block are regarded as training data with a large probability. In the case of homogeneous clutter, statistics of one clutter block data are even; the longer the block length is, the higher the accuracy of the coefficient estimates is, then, the shallower the frequency response notches are. For the details of SBLF structure, design, and optimization, see [11]. In the experiments below, the block length is the number to average SBLF coefficient estimates.

In the case of heterogeneous clutters, the transition boundaries' clutters from non-clutter to clutter or from strong to weak have different statistics, the coefficient estimates of a longer block may not reflect the statistics of them or their neighboring blocks. According to our experiments, the block length to average the estimates is selected between 20 and 30 bins.

3.4. Establishment of Clutter-Map

The clutter-map is a database that stores all information collected in the blocks Guard I Test, Test I, II into the corresponding map cell so to be invoked for reasoning, specifically the following five-class data. A range bin x a bearing bin point $z(t_n, l)$ of the return array forms a cell of the clutter-map. All the stored data are updated by the reasoning center as the new scan is finished:

1. The clutter levels, which are average magnitudes of the inputs of Test block and the outputs of Guard I, Test. Test I blocks with filtering-itself no matter a target presents inside or not.
2. The detection thresholds, which contain the output threshold and adaptive threshold from Test block.
3. The SBLF coefficients, which are calculated in Guard I block and used in Test block. The notch frequency parameters of the SBLF are also stored in the same map cell.
4. The target block index and terrace-indication index, which are set after block-delay or terrace-delay filtering in Test block and stored once the blocks are identified.
5. The PC output blip, whose level is recorded when the height is 8 dB higher than its both side clutters. The higher the blip is, the larger the probability of a target presenting in the blocks is.

3.5. Guidance of Stagger PRI

The SBLF processor is compatible with stagger PRI feature. This strategy designs many best PRIs under different conditions, which maintain the max improvement factors but whose notch positions are different. For example, one stagger-PRI suits for detecting targets lower than Mach 0.5 and the other PRI suits for targets higher than Mach 0.5. As soon as the SBLF coefficients are calculated, the notch frequency parameters of the SBLF are also determined. Even if the best stagger PRI is designed, there are always multi shallow notches, which can degrade the weak target acquisition. When the processor knows the notch is deep, e.g., -15 dB, it can suggest to agilely switch to the other stagger PRI that has different notches, then the Doppler frequency of the target may drop into or outside new notches in the alternative antenna bearing. If the new notch depth is -5 dB or shallower, the improvement factor will increase by 10 dB or larger.

In modern war, the electronic counter-measurement (ECM) is unavoidable. Hostile air reconnaissance always focuses on measuring radar parameters, including PRI; if the parameters are intercepted, the radar is easily attacked, then destroyed. The agile stagger PRIs also decrease the risk to be measured and attacked. Expect for the above strategies, the processor also contains a managing strategy, which is a manager to control the order of carrying out the strategies.

4. PERFORMANCES OF THE INTELLIGENT ADAPTIVE SBLF MTI PROCESSOR

In order to examine effectiveness of the SBLF processor, we select multi clutter models reflecting an S-band ship-borne radar environments [13] and carry out the simulation experiment like [14]. The generating clutters have two models: one is forested mountain plus windblown cloud, representing strong homogeneous clutter and the other is surging sea plus heavy raining, representing heterogeneous clutter [15]. The stagger PRI and large time-width PC features are involved. Two weak targets of high speeds are selected, and their Doppler parameters are listed on tops of the following figures. Two stagger codes are optimized, and stagger ratio is 1.23, blind-speed extension is 14.5; the average PRF is 720 Hz. The phase-coded PC is a minimum sidelobe 63-bit code of peak sidelobe 4 (−23.9 dB) [16]. The generating return arrays are of bearing bins 7 x range bins 240 and are divided into eight blocks of length 30 bins. The threshold factor $F_T = 1.6$ for homogeneous clutter and 1.7 for heterogeneous clutter. The terrace-indication declaration is with index sum 3. The adaptive threshold is calculated in terms of (1). White noise power is normalized to one, i.e., 0 dB.

The experimental results in the strong homogeneous clutter are showed in Fig. 4. The mountain clutter has P_g 60 dB, F_g 12 Hz, D_g 7.2 Hz and the cloud clutter, P_w 10 dB, F_w 240 Hz, D_w 58 Hz. The stagger-PRI code 27 26 31 29 30 28 32 is best within three times the average PRF. Fig. 4(a) shows target acquisition of the SBLF processor with a weak target (SCR -50 dB) of Mach 0.54. The blue input clutter completely submerges the target; the red SBLF output reveals a regular terrace-indication, indicating the clutter has been filtered out, which is of a length of 63 bins from 91 to 153 and about 24 dB height; at the black PC output, a target blip appears, about 60 dB high, whose position is just at bin 91, and the clutters at its both sides are fluctuating around 38 dB. The target-to-clutter ratio is about 22 dB, so the target dot will be brightly seen on the radar display screen. In Fig. 4(b), we also observe the performance of the SBLF processor with a very weak target (SCR −55 dB) of Mach 0.54. The red SBLF output curve reveals an irregular terrace-indication in place, fluctuating around 20 dB, and the clutters at its both sides are fluctuating around 15 dB, that is, the clutter is suppressed by about 45 dB. The black PC output is similar to that in (a) except for the blip of about 55 dB height and the clutters at the both sides are fluctuating around 37 dB. The target-to clutter ratio is about 18 dB, it is enough to see a bright target dot on the display. We figure out that the excellent performances of the SBLF processor in the homogeneous clutter results from three aspects: the real-time SBLF reaches optimal improvement factor, the target Doppler frequency does not drop into a frequency response notch and the heuristic strategies effectively control the reasoning operations.

For the simulation experiment in heterogeneous clutter, we also generate the clutter returns with stagger-PRI; the surging sea clutter has P_s 35 dB, F_s 24 Hz, D_s 48 Hz, and the heavy raining clutter has varying P_w from 20 to 45 dB, F_w 240 Hz, D_w 48 Hz. Stagger PRI code is 29 31 26 28 27

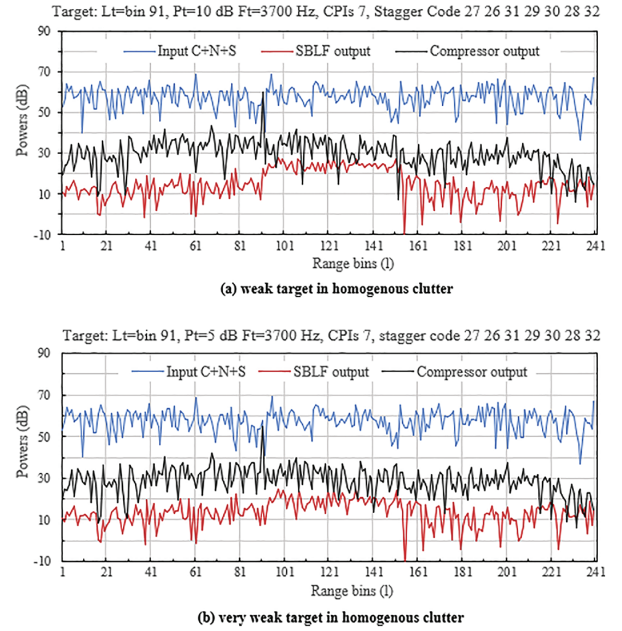


Fig. 4. Target acquisition of the SBLF processor on March 0.54 targets in strong land plus cloud clutters.

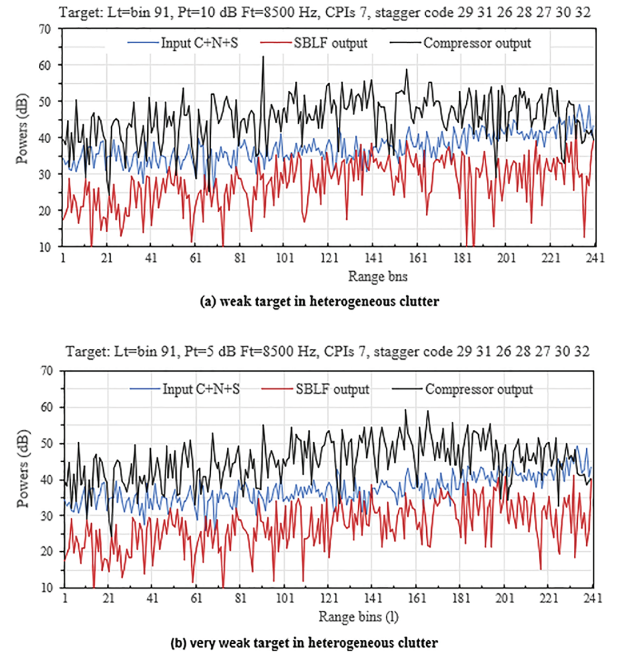


Fig. 5. Target acquisition of the SBLF processor on March 1.24 targets in sea plus varying raining clutters.

30 32 and the frequency response notches are shallowest within five times the average PRF. Fig. 5 shows the target acquisition of the SBLF processor with 10 dB weak target in (a) and 5 dB very weak target in (b), which both have very high speed, Mach 1.24. We observe that the two blue SBLF inputs are fluctuating around from 35 dB to 45 dB due to varying power of the raining clutter and the two targets are individually submerged in the clutter. In Fig. 5(a), the red SBLF output reveals an irregular terrace-indication in the range bins from 91 to 153, fluctuating around 33 dB, not clearly visible, the clutters at both sides of the terrace are fluctuating around 26 and 33 dB, respectively and the clutter is suppressed by about 10 dB only due to

the quite wide band clutters; the black PC output has a target blip in place, about 63 dB high, the clutters at its both sides are about 49 dB, 14 dB lower than the blip. In Fig. 5(b), the red SBLF output curve is similar to that in (a) except for an almost invisible terrace-indication at bins 91 to 153 due to dominated clutter, fluctuating around 29 dB; however, the processor still identifies the hidden terrace-indication with its indices 3; the black PC output is also similar to that in (a) except for the target blip, about 56 dB high and 9 dB higher than its side clutters. We figure out that in the severe heterogeneous clutters plus the weak targets, SCRs -35 and -40 dB, the processor can acquire the weak targets because the SBLF coefficients have still optimal improvement and the target Doppler frequency does not drop into the blind speed notches; additionally, the heavy raining clutter has varying power and wide frequency band, but its max power is not strong, 45 dB. In order to improve the processor for better performance in heterogeneous clutter, more priori knowledges need to be dug out.

5. SUMMARY

Through many experiments on the target acquisition in generating homogeneous and heterogeneous clutters, the performance of the adaptive SBLF processor without artificial intelligence can not meet the requirement of nowadays MTI radars and the approach of using optimized algorithms only has been outdated:

1. An early MTI processor only utilized a simple arithmetic operation but a nowadays adaptive MTI processor involves multi advanced technologies, such as adaptive filtering, large time-wide PC, stagger PRI, etc. The compatibility problems, such as how the training data are realized in the adaptive operation, how the PC waveform is identified after SBLF filtering, and how an adaptive threshold is set up for homogeneous and heterogeneous clutters, all solutions need reasoning operations, such as learning, analyzing, etc. rather than optimal algorithm only. The intelligent operations rely on the priori knowledges of radar professionals, which involve the radar environmental clutters, SBLF response notches formed by stagger-PRI, radar DSP processing computer logic language/syntaxes, etc. We propose the reasoning center of the processor, which can be used for target identification, adaptive threshold set-up, and PC terrace-indication; our experiments illustrates that they are valid for the weak-target acquisition. The real-time SBLF is the core of optimal clutter suppression and the reasoning center is the core of the intelligent operations; the combination of both comprises an intelligent adaptive SBLF MTI processor.
2. In order to ensure the intelligent operations of the SBLF processor to be valid, we do many simulation experiments, then propose five heuristic strategies.
 - ① Non-clutter input decision and adaptive threshold set-up, which decides if Test block input is

enough weak to disable SBLF in the block; secondly, the filtering-itself outputs of several blocks are used to set up the detection threshold for target block identification. ② Target block identification and terrace-indication declaration, which creates the rule for the adaptive threshold to identify target presence and setting target block index, and the rule for declaring terrace-indication of PC target and setting terrace-indication index. ③ SBLF coefficient estimation, which calculates the SBLF coefficients based on the realized training data in Guard I block and loads the coefficients to Test block. ④ Establishment of clutter-map, which stores the adaptive thresholds, target block indices, terrace-indication indices, PC output blip levels, and frequency parameters of notches. All the data are stored in the corresponding clutter-map cells and are updated and invoked as the reasoning references. ⑤ Guidance of stagger-PRI, which provides multi stagger PRI codes for the MTI to agilely prevent the target speed from dropping into a deep notch and for radar to decrease risk of electronic counter-measurement; the max blind-speed extension of stagger PRI is 14.5. The strategy expression of the adaptive SBLF processor uses FORTRAN syntax.

3. In our simulation experiments to illustrate the SBLF processor performances, the homogeneous and heterogeneous clutters are selected to reflect forested mountain plus windblown cloud and surging sea plus varying heavy raining, respectively. The stagger PRI codes are optimized by arranging the integers 26 27 28 29 30 31 32, the average PRF is 720 Hz, and the stagger ratio is 1.23; the 63 bits, minimum sidelobe phase-coded PC is involved. The return array of number of the CPI pulses 7 and range length 240 bins is selected and divided into 8 blocks. The real-time SBLF is compatible with stagger PRI; the five heuristic strategies are applied. From the results, we conclude that in the homogeneous clutter the strong inputs submerge the weak targets of Mach 0.54, SCRs -50 , -55 dB, the SBLF outputs present regular terrace-indications, and two target blips at PC outputs have SCRs 22 and 18 dB. The weak target outside of notch and medium target dropping into notch can be acquired. Such excellent performance can not be reached without the intelligent operations. We also illustrate the performance in the heterogeneous clutter and the same weak targets of Mach 1.24. The SBLF outputs present irregular terrace-indications but the PC outputs exhibit the target blips in place. The target acquisitions of SCRs 14 dB and 9 dB are good; however, it is still required for us to continue researching the weak target acquisition under the heterogeneous condition.

CONFLICT OF INTEREST

The authors declare that they do not have any conflict of interest.

REFERENCES

- [1] Zhang W, Ma S, Du Q. Optimization of adaptive MTI filter. *Int J Commun, Netw Syst Sci.* 2017;10:206–17.
- [2] Haykin S. *Adaptive Filter Theory*. 5th ed. Edinburgh Gate, London: © Pearson Education Limited; 2014, pp. 150–208.
- [3] Thurber RE. Advanced signal processing techniques for the detection of surface targets. *Johns Hopkins Univ Appl Phys Lab.* 1983;4(4):285–95. Available from: <https://secwww.jhuapl.edu>.
- [4] Gaby JH, Hayes MH. Artificial intelligence applied to spectrum estimation. *The 1984 International Conference on Acoustics, Speech, and Signal Processing*, pp. 13.5.1–4, San Diego, USA, 1984.
- [5] Gass WS, Tarrant RT, Pawate BI, Gammel M, Rajasekaran PK, Wiggins RH, *et al.* Multiple digital signal processor environment for intelligent signal processing. *Proc IEEE.* 1987;75(9):1246–59.
- [6] Wicks MC, Melvin WL, Chen P. An efficient architecture for non-homogeneity detection in space-time adaptive processing airborne early warning radar. *Proceedings of the 1997 International Radar Conference*, pp. 295–9, Edinburgh, UK, 1997.
- [7] Melvin WI, Guerci JR. Knowledge-aided signal processing: a new paradigm for radar and other advanced sensors. *IEEE Trans Aerosp Electron Syst.* 2006;42(3):938–96.
- [8] Wicks MC, Rangaswamy M, Adve R, Hale TB. Space-time adaptive processing. [A knowledge-based perspective for airborne radar]. *IEEE Signal Process Mag.* 2006;Jan:51–65.
- [9] O'Donnell RM. *Introduction to Radar Systems Clutter Rejection MTI and Pulse Doppler Processing*. MTI Lincoln Laboratory; 2001. Available from: <https://www.ll.mit.edu> > media.
- [10] Allen C. Radar Pulse Compression. 2004. Available from: <https://www.mathworks.com> > help > signal.
- [11] Zhang X. Lattice predictors for stagger-period sequence: their theory and application. *Sci PC J Electr Electron Eng.* 2022;10(5):184–98.
- [12] Zhang X. Finite impulse response filters for stagger-period signals, their designs and applications. *Eur J Inf Technol Comput Sci.* 2021;1(1):1–11.
- [13] Subramaniam CH. *Shipborne Radar and ARPA*. 3rd ed. Mumbai, India: Publications V; 2001 Nov, pp. 1–78.
- [14] Lu D. *Simulation and Verification of Pulse Doppler Radar Systems Application Note*. USA: Agilent Technologies Inc; 2010. www.agilent.com/find/radar.
- [15] Zhang X. New methods of simulating radar clutter return arrays. *EJECE, Eur J Eng Comput Sci.* 2023;7(6):46–57.
- [16] Greg C, Jon R. Efficient exhaustive search for optimal-peak-sidelobe binary codes. *IEEE TRANS AES.* 2005;41(1):302–8.